

## Effect of a metallic gate on the energy levels of a shallow donor

A. F. Slachmuylders,<sup>1,a)</sup> B. Partoens,<sup>1</sup> F. M. Peeters,<sup>1</sup> and W. Magnus<sup>1,2</sup>

<sup>1</sup>Departement Fysica, Universiteit Antwerpen, Groenenborgerlaan 171, B-2020 Antwerpen, Belgium

<sup>2</sup>Interuniversity Microelectronics Centre, Kapeldreef 75, B-3001 Leuven, Belgium

(Received 21 November 2007; accepted 5 February 2008; published online 26 February 2008)

We have investigated the effect of a metallic gate on the bound states of a shallow donor located near the gate. We calculate the energy spectrum as a function of the distance between the metallic gate and the donor and find an anticrossing behavior in the energy levels for certain distances. We show how a transverse electric field can tune the average position of the electron with respect to the metallic gate and the impurity. © 2008 American Institute of Physics. [DOI: 10.1063/1.2888742]

The study of shallow donor impurities near an interface has gained renewed interest in view of the perspective toward atomic scale electronics. On one hand, a very promising application consists of the realization of a qubit exploiting shallow donor states as was initially proposed by Kane<sup>1</sup> for a P dopant in Si. To manipulate (readout) the qubit, one proposes the use of a metallic gate to control the position of the electron.<sup>2</sup> On the other hand, controlling donor states is equally important to pursue the miniaturization of nanodevices, e.g., transistors having only a few dopants in their conduction channel. Recently, Sellier *et al.*<sup>3</sup> have studied the effect of an impurity on the electrical transport in a semiconductor nanowire. As three-dimensional (3D) atomical control of the dopant position has already been realized,<sup>4</sup> a better understanding of the physics of single dopant is highly desirable to anticipate future applications in nanoelectronics. In the first part of this letter, we study the energy levels of a single dopant, which provide useful information for transport experiments. The obtained energy levels indicate where tunneling through the donor site can occur, since tunneling is invoked when the applied gate voltage causes the dopant energy level to match with the Fermi level in source and drain. For both qubit and transport applications, a good knowledge of the low-energy spectrum is required, which is determined by the anticrossing. Therefore, it is justified to have a closer look at it and its peculiarities. In the second part of the paper, we investigate how the electric field can be used to tune the electron position between the donor site and the interface.

In previous theoretical work,<sup>2,5–8</sup> the properties of a donor placed near a thick insulating interface were studied. In this constellation, the dielectric mismatch (e.g.,  $\epsilon_{\text{Si}} = 11.9$  and  $\epsilon_{\text{SiO}_2} = 3.4$ ) leads to an enhancement of the Coulomb interaction. The gate was assumed to be sufficiently far away from the interface to prevent screening while merely providing an electric field to drive the electron away from the impurity. Here, we consider the opposite case of a very thin oxide layer separating the metallic gate from the semiconductor (see inset of Fig. 1). The oxide layer negligibly contributes to the dielectric mismatch but only prevents the electron from leaving the semiconductor. The metallic gate not only screens the Coulomb potential but also provides an electric field which tunes the electron position. We consider a donor located at a distance  $d$  from a semiconductor/insulator/metal

interface. In accordance with the experimental setup described in Ref. 3, we assume that the thickness of the insulator is negligibly small. Moreover, its potential barrier is considered infinitely high so as to confine the electron to the semiconductor region. Due to dielectric mismatch effects—the permittivity  $\epsilon_1$  at the semiconductor side of the interface is typically of the order of 10, while the permittivity  $\epsilon_2$  of the metallic gate is infinite—image charges will arise that screen the interaction potential between the impurity and the electron. The potential energy  $W$  between an electron and an impurity near the semiconductor/metal interface at position  $\vec{r}_h = (0, d)$  is given by<sup>9</sup>

$$W(\vec{r}_e, \vec{r}_h) = \frac{e^2}{4\pi\epsilon_1} \left[ -\frac{1}{4z_e} - \frac{1}{\sqrt{\rho_e^2 + (z_e - d)^2}} + \frac{1}{\sqrt{\rho_e^2 + (z_e + d)^2}} \right], \quad (1)$$

with  $\rho = \sqrt{x^2 + y^2}$ . The first term arises from the interaction between the electron and its image, the second term is due to the normal electron-impurity interaction, whereas the last term represents the interaction between a particle (electron or impurity) and the image of the other particle (impurity image or electron image). The impurity-impurity image interaction is removed, since it merely amounts to a constant energy shift. The potential energy profile exhibits a double well structure (see Fig. 1, where  $W$  is plotted for two impurity positions  $d/a_d$ , with  $a_d = (4\pi\epsilon_1\hbar^2)/(m_{\perp}e^2)$  the donor Bohr radius,  $m_{\perp}$  the transverse effective mass, and  $W_0 = e/(4\pi\epsilon_1 a_d)$ ). When the impurity moves toward the inter-

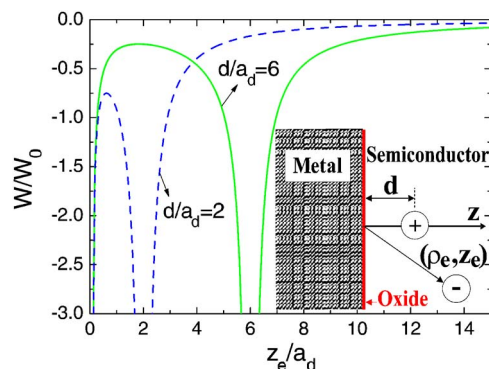


FIG. 1. (Color online) Plot of the electron energy along the  $z$  axis ( $\rho_e = 0$ ) for two different impurity positions. Note that  $W_0 = e^2/(4\pi\epsilon_1 a_d)$  and  $a_d = 4\pi\epsilon_1\hbar^2/(m_{\perp}e^2)$ . Inset: schematical representation of the studied system.

<sup>a)</sup>Electronic mail: an.slachmuylders@ua.ac.be.

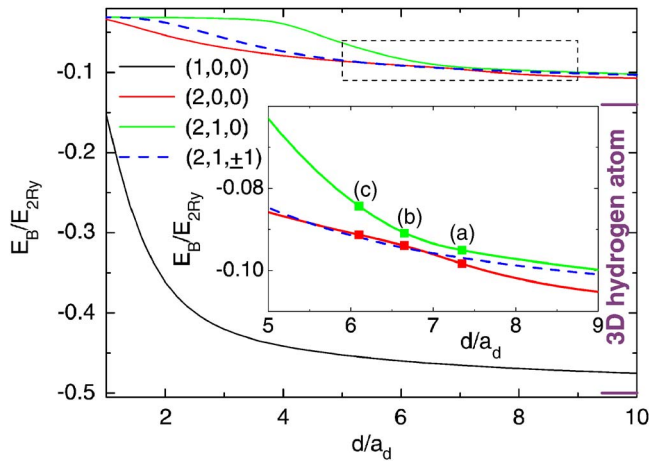


FIG. 2. (Color online) Energy spectrum vs the donor position  $d/a_d$  with respect to the metallic interface. The values for the 3D hydrogen atom are indicated at the right of the figure. Inset: box region indicated by the dotted curves in the main figure.

face, the potential wells start to interact strongly and eventually combines into a single well. Exploiting the cylinder symmetry of the problem, we may write the dimensionless Hamiltonian of the system as<sup>5</sup>

$$H = -\frac{1}{2} \left[ \frac{\partial^2}{\partial \rho_e^2} + \frac{1}{\rho_e} \frac{\partial}{\partial \rho_e} - \frac{m^2}{\rho_e^2} + \gamma \frac{\partial^2}{\partial z_e^2} \right] + \left[ -\frac{1}{4z_e} - \frac{1}{\sqrt{\rho_e^2 + (z_e - d)^2}} + \frac{1}{\sqrt{\rho_e^2 + (z_e + d)^2}} \right] + \tilde{F}z, \quad (2)$$

where  $\gamma = m_{\perp}/m_{\parallel}$  is the ratio between the transverse and longitudinal effective masses (for simplicity, we took  $\gamma = 1$  in our calculations). Because of the cylindrical symmetry, we have  $\Psi_e = e^{im\theta_e} \psi(\rho_e, z_e)$ . We introduced the donor Bohr radius  $a_d$  as the unit of length and twice the Rydberg energy,  $E_{2Ry} = \hbar^2/(m_{\perp} a_d^2)$  as the unit of energy.  $\tilde{F} = F/F_0$ , where  $F$  is a uniform electric field and  $F_0 = E_{2Ry}/(ea_d)$ . For Si, the atomic units are  $a_d = 3.31$  nm,  $E_{2Ry} = 36.5$  meV, and  $F_0 = 110$  kV/cm, whereas for GaAs we find  $a_d = 9.89$  nm,  $E_{2Ry} = 11.6$  meV, and  $F_0 = 12$  kV/cm. Notice that the Hamiltonian given in Eq. (2) corresponds to a (scaled) hydrogen model for large values of  $d/a_d$ .

Using finite element techniques, we obtained a numerically exact solution to the effective two-dimensional Schrödinger equation. The resulting energy levels for  $F/F_0 = 0$  are shown in Fig. 2 where we labeled the energy levels with  $n$ ,  $l$ , and  $m$ . Due to cylindrical symmetry, only  $m$ , the quantum number of the angular momentum operator  $L_z$ , is conserved in contrast to  $n$  and  $l$ , the quantum numbers of the  $d/a_d \rightarrow \infty$  hydrogen spectrum. For large values of  $d/a_d$ , the energy levels are seen to converge to the hydrogenic energy levels  $E_n = \hbar^2/(2m_{\perp} a_d^2 n^2)$ , as was to be expected. One can clearly see an anticrossing behavior between the  $(n, l, m) = (2, 0, 0)$  and  $(2, 1, 0)$  energy levels (levels of equal  $m$  and originating from different  $l$  quantum numbers) for  $d/a_d \approx 6.6$ . The surrounding region is enlarged in the inset of Fig. 2 where it is seen clearly that both levels fail to interact with the  $(2, 1, 1)$  level due to a different quantum number  $m$ . Similar observations can be made for other parts of the spectrum. Near the anticrossing, the probability densities (see Fig. 3) undergo drastic changes: the probability density of the

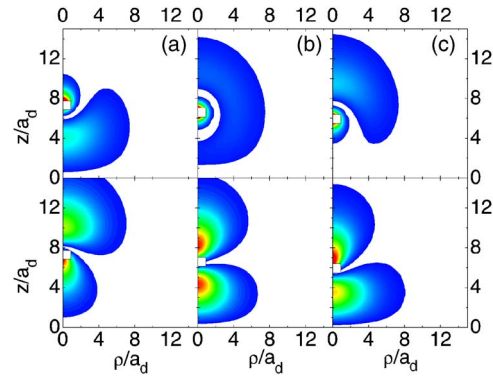


FIG. 3. (Color online) Probability density in (a), (b), and (c) as indicated in the inset of Fig. 2 as function of the distance  $d/a_d$  from the metallic interface. The top three figures correspond to the densities of the  $(2,0,0)$  energy level, whereas the three figures at the bottom correspond to the  $(2,1,0)$  energy level. The donor position is indicated by the white square. Blue (red) areas represent low (high) probabilities. The white area represents zero probability.

$(2,0,0)$  level exhibits a secondary extremum first underneath, then around and finally above the primary extremum with decreasing  $d/a_d$ . As  $d/a_d$  decreases, the  $(2,1,0)$  probability density shows an increase in size of the bottom lobe, which explains the energy increase since the corresponding  $p_z$ -like orbital piles up against the interface. We did not plot the probability density of the  $(2,1,1)$  state, since it does not interact with any other state and no significant changes in the shape of the wave function are found.

Next, we investigated the possibility of using of an electric field to influence the position of the electron. For quantum computing purposes, such an electric field can be used to move the electron back and forth between the donor site and the interface. From Fig. 4, it is clear that an increasing field pushes the electron closer to the interface for all donor positions. For larger values of  $d/a_d$  (e.g.,  $d/a_d = 10$ ), a weak electric field is already sufficient to considerably enlarge the distance from the donor position; indeed, for  $d/a_d = 10$ , the average distance of the electron  $\langle z \rangle/a_d$  approximately equals 2.4 for  $F/F_0 = 0.1$ , whereas for  $F/F_0 = 0$ , we find  $\langle z \rangle/a_d = 10$ . If the donor is closer to the interface, a larger electric field is required to pull the electron away from the donor site [e.g., see Fig. 4 and consider  $F/F_0$  for  $\langle z \rangle/a_d = (d/a_d)/2$ ]. However, for an efficient manipulation of the electron states in a

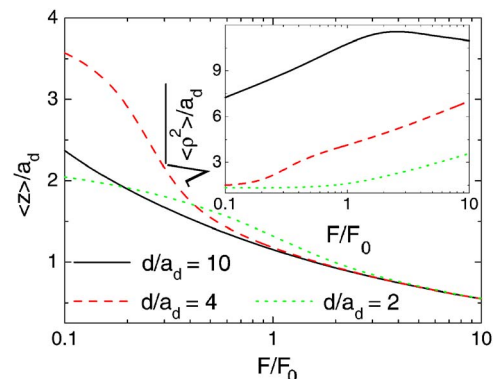


FIG. 4. (Color online) Expectation value of the electron position along the  $z$  axis,  $\langle z \rangle/a_d$ , as a function of the electric field for different impurity positions. Inset: expectation value of the electron wave function extending along the  $(x, y)$  plane,  $\sqrt{\langle \rho^2 \rangle}/a_d$ , as a function of the electric field for different impurity positions.

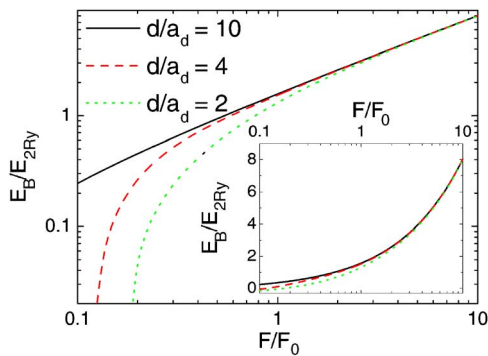


FIG. 5. (Color online) Log-log plot of the ground state energy levels for  $m=0$  as a function of the electric field for different impurity positions. Inset: same but now with a linear scale for the energy.

real quantum device, it is compulsory that switching the electron between the interface and the donor site be completely reversible. Therefore, the electron state near the interface should remain laterally bound to its donor site. However, from the inset in Fig. 4, we notice that while an increasing electric field drags the electron toward the interface, the lateral localization of the electron wave function is found to deteriorate. This negative effect obviously restricts the allowed range of minimal interdonor distances.

Finally, the ground state energy was calculated as a function of the electric field for different donor positions. Figure 5 shows that for larger electric fields the energies are independent of the donor position, i.e., the electric field is strong enough to pull away the electron from the impurity site for any value of  $d/a_d$ .

To conclude, in this letter, we investigated the energy levels of an impurity near a metallic interface. We calculated

the energy levels of the impurity as a function of the donor position and compared them with the bulk values to demonstrate the effect of the metallic interface on the energy levels that may also carry source-to-drain tunneling currents in nanoscale transistors. In view of potential quantum computing applications, we have studied the effect of an electric field moving the electron away from the donor site to the interface. In order to maintain an acceptable degree of lateral localization of the electron at the interface only low electric fields are allowed to switch between the donor site and the metallic interface. This conclusion is also supported by the electric field dependence of the energy spectrum: if the electric field becomes too large, the energy spectrum is dominated by the electric field strength and not by the characteristic of the sample, e.g., the donor position.

This work was supported by the UA-IMEC, vzw collaborative project, the Belgian Science Policy (IAP), and the EU network of excellence: SANDiE.

<sup>1</sup>B. E. Kane, *Nature (London)* **393**, 133 (1998).

<sup>2</sup>M. J. Calderón, B. Koiller, X. Hu, and S. Das Sarma, *Phys. Rev. Lett.* **96**, 096802 (2006).

<sup>3</sup>H. Sellier, G. P. Lansbergen, J. Caro, and S. Rogge, *Phys. Rev. Lett.* **97**, 206805 (2006).

<sup>4</sup>F. J. Rueß, W. Pok, T. C. G. Reusch, M. J. Butcher, K. E. J. Goh, L. Oberbeck, G. Scappucci, A. R. Hamilton, and M. Y. Simmons, *Small* **3**, 563 (2007).

<sup>5</sup>D. B. Macmillan and U. Landman, *Phys. Rev. B* **29**, 4524 (1984).

<sup>6</sup>H. Sun and S.-W. Gu, *Phys. Rev. B* **46**, 2244 (1992).

<sup>7</sup>A. S. Martins, R. B. Capaz, and B. Koiller, *Phys. Rev. B* **69**, 085320 (2004).

<sup>8</sup>M. J. Calderón, B. Koiller, and S. Das Sarma, *Phys. Rev. B* **75**, 125311 (2007).

<sup>9</sup>D. J. Griffiths, *Introduction to Electrodynamics*, 2nd ed. (Prentice-Hall, India, 1989), p. 124.